2D Mater.

2×2 Charge Density Wave in single-layer $TiTe_2$

Bogdan Guster[1], Roberto Robles[1], Miguel Pruneda[1], Enric Canadell[2], Pablo Ordejón[1]

[1]Catalan Institute of Nanoscience and Nanotechnology (ICN2), CSIC and BIST, Campus UAB, Bellaterra, 08193 Barcelona, Spain
[2]Institut de Ciència de Materials de Barcelona (ICMAB-CSIC), Campus Bellaterra, 08193 Barcelona, Spain

E-mail: pablo.ordejon@icn2.cat

Abstract. A density functional theory study concerning the origin of the recently reported 2×2 charge density wave (CDW) instability in single-layer $TiTe_2$ is reported. It is shown that, whereas calculations employing the semi-local functional PBE favor the undistorted structure, the hybrid functional HSE06 correctly predicts the 2×2 distortion, . The study suggests that the magnitude of the semi-metallic overlap between the valence band top at Γ and the conduction band bottom at M is a key factor controlling the tendency towards the distortion. It is also shown that tensile strain stabilizes the 2×2 CDW, and we suggest that this fact could be further used to induce the instability in double-layers of $TiTe_2$ which in the absence of strain remain undistorted. The driving force for the CDW instability seems to be the same phonon mediated mechanism acting for single-layer $TiSe_2$, although in single-layer $TiTe_2$ the driving force is smaller, and the semimetallic character is kept below the transition temperature.

Keywords: Single layer dichalcogenides, charge density waves, density functional theory, exchange-correlation funtionals, titanium ditelluride, 2D materials.

1. Introduction

Transition metal dichalcogenides of the groups IV and V rank among the most controversial materials exhibiting charge density wave (CDW) instabilities [1, 2]. The possibilities of strong or weak electron-phonon coupling scenarios in group V $2H$-MX_2 (M = Nb, Ta; X = S, Se) and either phonon mediated or excitonic mechanisms in group IV $1T$-$TiSe_2$ have been discussed for decades [1]. Many of these systems also exhibit superconductivity (SC) under certain conditions and the competition between the two instabilities remains an important question still unanswered [3, 4]. These materials are built from MX_2 layers interacting through weak van der Waals forces and thus are easily exfoliated [5]. Consequently, they offer the possibility to examine the above mentioned issues at the two-dimensional (2D) limit as well as by smoothly varying the density of carriers through gate doping. This is at the origin of the huge revival of interest recently raised by these materials [6, 7, 8, 9, 10, 11].

Indeed, intriguing differences of these few-flake or even single-layer materials with their bulk counterparts have been discovered. Recent reports on the existence of a very weak pseudo-gap at the Fermi energy in single-layer $NbSe_2$ [6, 12] or the possible occurrence of incommensurate modulations for slightly electron doped $TiSe_2$ crystals of thicknesses less than 10 nm [10, 13] make clear that we are still far from a full understanding of the physics of CDW materials and more particularly when the screening is reduced.

In this context, the recent report of a 2×2 CDW in single-layer $TiTe_2$ by Chen *et al.* [8] came as a very intriguing surprise. Since long [14, 15, 16] it has been known that bulk $1T$-$TiTe_2$ does not exhibit the 2×2 CDW that occurs in isostructural $1T$-$TiSe_2$ [17] In addition, the 2×2 CDW is not observed anymore in double-layer $TiTe_2$ [8]. In contrast, the 2×2 CDW instability is observed in $TiSe_2$ from the single-layer, for ultrathin films with up to six layers [18], and for the bulk crystal [17]. The experimental indication of the occurrence of the CDW in single-layer $TiTe_2$ is even more surprising when considering that first-principles density functional theory (DFT) calculations found that single-layer $TiTe_2$ shows no tendency to distort towards the 2×2 CDW structure at the generalized gradient approximation (GGA) level [8]. Yet, calculations of the same quality successfully predict that the 2×2 CDW structure is more stable than the non-distorted structure for single-layer $TiSe_2$ [18, 19, 13]. Overall, these observations suggested the hypothesis that something really new and challenging is at work in single-layer $TiTe_2$ [8].

However, one should note that the CDW transition occurs at 100 K in single-layer $TiTe_2$ [8] but at a considerably higher temperature, 232 K, in single-layer $TiSe_2$ [11]. Hence, the driving force for the distortion must be considerably weaker in single-layer $TiTe_2$. Before concluding that a new scenario is needed to grasp the origin of the unexpected 2×2 CDW in this material, one should wonder about the appropriateness of the so far successful GGA-type of DFT approaches to the CDW instabilities in single-layer group IV and V dichalcogenides. Such an appraisal is needed because it impinges on very fundamental questions concerning CDW instabilities at the 2D limit. Note that it has been recently shown [20] that GGA-type functionals like PBE [21] overestimate the overlap between the Ti $3d$ and Se $4p$ levels in bulk $1T$-$TiSe_2$. This can be corrected by using hybrid functionals like HSE06 [22, 23] leading to an improvement of the electronic description of bulk $TiSe_2$ [20]. In the following we report a DFT study of the likeliness of a 2×2 CDW in single-layer $TiTe_2$ employing both PBE and HSE06 functionals which provides useful insight on the origin of the CDW instability in single-layer $TiTe_2$.

2. Results and Discussion

An isolated layer of $1T$-$TiTe_2$ is made of an hexagonal lattice of Ti atoms in an octahedral environment of Te atoms (Fig. 1a). The repeat unit of the hexagonal bulk crystal structure contains just one of these layers. A detailed description of our calculation method is presented in Appendix A. Let us start our analysis by briefly considering the PBE description of the electronic structure. The optimized a cell parameter is 3.804 Å for the single layer and 3.815 Å for the bulk, in good agreement with the bulk experimental value of 3.777 Å [24]. Within a single-layer there are several Te...Te contacts shorter than the sum of the van der Waals radii so that the valence bands, which have their maximum at Γ and are mostly built from Te $5p$ orbitals, are considerably wide and overlap with the bottom part of the Ti $3d$ bands, which have their minima at the M point (Fig. 1b). As expected from the fact that in the bulk there are short Te...Te

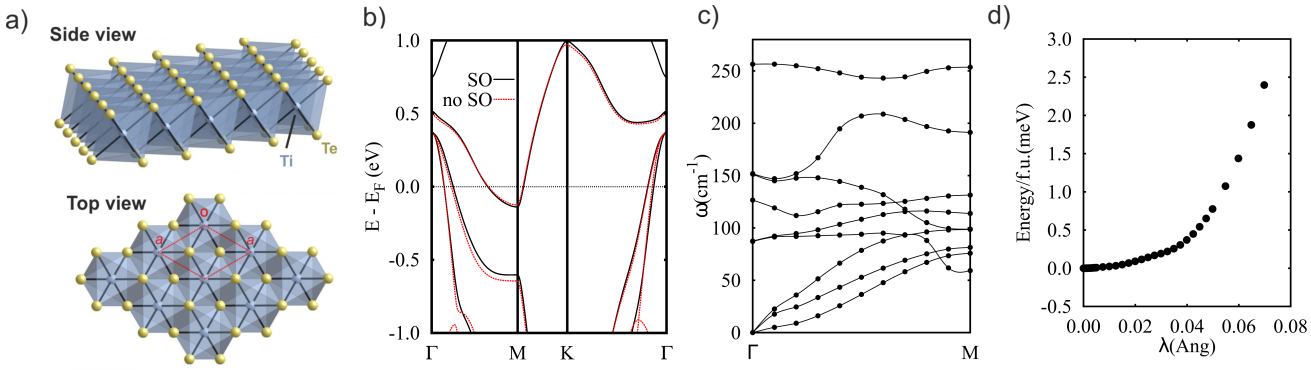

Figure 1. Single-layer $TiTe_2$. (a) Side and top views of a layer. (b) Calculated GGA band structure with (black lines) and without (red dots) spin-orbit coupling. Γ = (0, 0, 0), M= (1/2, 0, 0) and K= (1/3, 1/3, 0) in units of the reciprocal hexagonal lattice vectors. (c) GGA phonon dispersion in the Γ - M segment of the Brillouin Zone (BZ) for the undistorted structure. (d) Frozen-phonon total energy calculation as a function of the soft phonon mode amplitude at M, calculated with the GGA functional. Energies are given in meV per formula unit relative to the undistorted phase. All results have been obtained using the PBE functional.

contacts in the direction perpendicular to the layer, the semimetallic overlap is 19% larger in the bulk. Note that, as it is clear from Fig. 1b, inclusion of spin-orbit coupling effects does not have any noticeable effect and therefore it will not be considered anymore in the following. Thus, according to the PBE calculations single-layer $TiTe_2$ is a semimetal exactly as the bulk. In contrast with the case of single-layer $TiSe_2$, for which the same type of calculations led to a phonon with imaginary frequency at the M point [13], our calculations with the GGA functional for single-layer $TiTe_2$ (Fig. 1c) show no phonons with imaginary frequency, in agreement with those of Chen *et al.* [8]. Although there is some remnant of the instability at M (notice the optical branch that disperses downwards and shows the lowest frequency at the M point, reminiscent of the mode that becomes unstable for $TiSe_2$), there is no definite indication of a phonon instability that may lead to the 2×2 distortion of the structure. Detailed structural optimizations of 2×2 supercells confirmed this result. However, as indicated by the frozen-phonon total energy calculation as a function of the soft phonon mode amplitude at M (Fig. 1d), the GGA potential energy surface is extremely flat. Under such circumstances, even if strictly speaking the PBE calculations disagree with the experimental results in that no tendency toward the 2×2 CDW distortion is found, the results are somewhat inconclusive and a closer look is needed.

The very flat frozen-phonon energy curve of Fig. 1d) suggests that small external perturbations could be able to change the relative stability of the undistorted and 2×2 CDW structures. This could occur, for instance, by the effect of strain. Thus, we studied the evolution of the band structure and the relative stability of the undistorted 1×1 and 2×2 CDW structures as a function of biaxial tensile strain (allowing the atomic positions to relax for each strain applied). The strain is defined as $s = \delta m/m_0$ where m_0 is the unstrained cell parameter and $\delta m + m_0$ the strained cell parameter. Thus, positive values correspond to tensile strains. As shown in Table 1, a tensile stress as small as 1% is sufficient to make the 2×2 CDW structure slightly more stable than the undistorted one. For strains larger than 2%, the 2×2 CDW is definitely favored. When this happens, energy gaps open at the crossings of the folded valence and conduction bands although, as shown in Fig. 2, the distorted structure is still semimetallic and only for relatively large tensile strains (between 5 and 6%) a clear band gap occurs around the Fermi level. Thus, it appears that GGA-PBE description of single-layer $TiTe_2$ is only consistent with the the real situation when a slight tensile strain in imposed in the calculation. The main effect of the strain is a decrease of the intralayer Te...Te short contacts which leads to a decrease of the Te $5p$ bandwidth

Table 1. Evolution with tensile strain of: (i) the energy difference between the undistorted structure and the relaxed 2×2 CDW structure, and (ii) displacement of the Ti atoms in the plane parallel to the layer from their position in the undistorted phase. All values obtained using the PBE functional.

Tensile Strain (%)	ΔE (meV/f.u.)	Δ Ti(Å)
0	0.00	0.000
1	-0.001	0.007
2	-0.09	0.057
3	-0.29	0.061
4	-0.47	0.067
5	-0.74	0.080
6	-1.27	0.095
7	-2.04	0.118

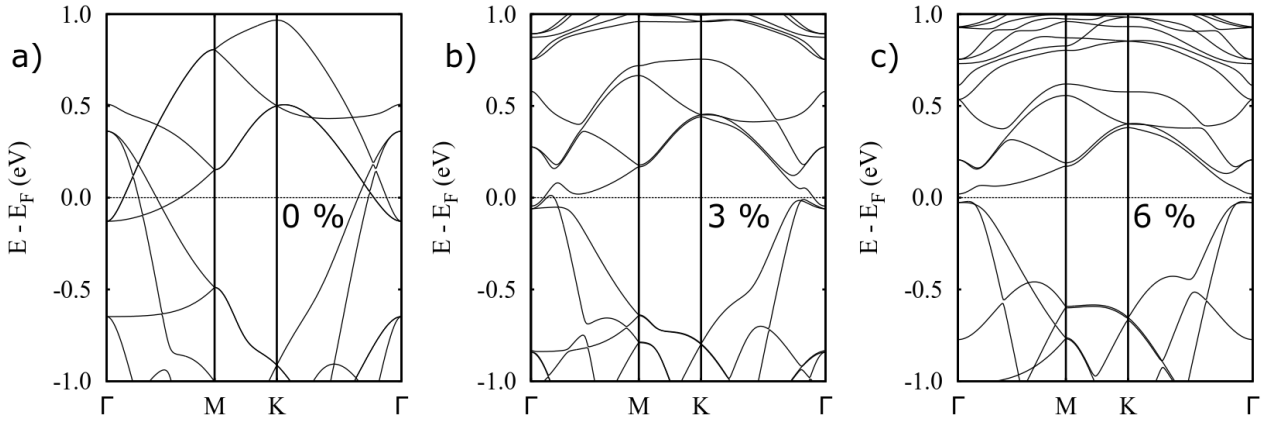

Figure 2. Calculated GGA band structures for the stable 2×2 CDW structure of single-layer $TiTe_2$ under tensile biaxial strain calculated with the PBE functional: (a) 0%, (b) 3% and (c) 6% biaxial strain. Γ = (0, 0, 0), M = (1/2, 0, 0) and K = (1/3, 1/3, 0) in units of the reciprocal hexagonal lattice vectors.

and, consequently, of the semimetallic overlap. Only when this overlap decreases with respect to the PBE description of the system the 2×2 CDW becomes more stable. This observation is consistent with the fact that when Te...Te interlayer interactions come into play in the bulk or even in the double-layer, the semimetallic overlap increases and the 2×2 CDW is not observed anymore.

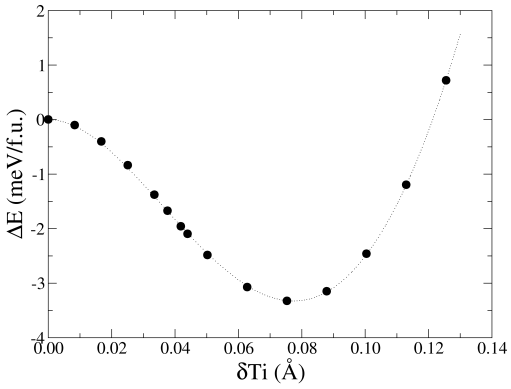

Figure 3. Energy difference (in meV per formula unit) between the undistorted and 2×2 CDW structures of an unstrained $TiTe_2$ single-layer according to DFT calculations using the hybrid HSE06 functional

These results are reminiscent of the above mentioned work concerning the functional type dependence of the semimetallic overlap of bulk $TiSe_2$ [20] and prompted us to reconsider the stability of the unistorted vs. 2×2 CDW structures using the hybrid type functional HSE06 [22, 23]. Shown in Fig. 3 is a frozen-phonon calculation of the energy difference between the undistorted structure and the 2×2 CDW structure following the soft phonon mode distortion. The curve clearly shows that, at the HSE06 level, unstrained single-layer $TiTe_2$ is indeed unstable towards the 2×2 CDW distortion. By relaxing the structure around the minimum of the frozen-phonon curve we have obtained an energy gain of 3.8 meV/formula unit. This stabilization energy is much lower than the value obtained for a $TiSe_2$ monolayer using a PBE functional, 6 meV/f.u [13]. Hellgren *et al.* [20] showed that for bulk $TiSe_2$ hybrid functionals predict a much higher stabilization energy than the PBE functional. Thus, it is understandable that according to our PBE type studies single-layer $TiTe_2$ does not tend to experience a 2×2 CDW instability. Overall, our data suggest a weak driving force for the distortion.

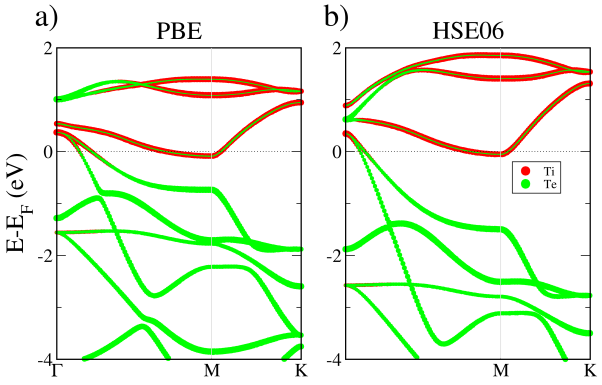

Figure 4. Calculated band structure for $TiTe_2$ single-layer using the PBE (a) and hybrid HSE06 (b) functionals. The size of the green and red circles is proportional to the Te and Ti character, respectively.

Since this is a significant result let us consider in more detail the region of the semimetallic overlap. A fatband analysis of the PBE and HSE06 band

structures is shown in Figs. 4a and b, respectively. A close inspection at the region around Γ points out some clear differences between the results of both functionals. For PBE, above the (partially empty) top of the valence band at Γ there is a non-degenerate band and a pair of degenerate bands at a higher energy. The order is the opposite for the HSE06 functional (Fig. 4b), for which the two degenerate bands are lower in energy. Around the Fermi level a heavy mixing of the t_{2g} levels of the Ti atom and the $5p$ levels of the Te atoms occurs. Assuming a local coordinate system in which the three-fold symmetry axis of the octahedron occurs along the z direction, the non-degenerate Ti-based band is essentially built from the Ti d_{z^2} orbital, whereas the top of the valence band, which is doubly degenerate at Γ, is mainly built from the Ti $d_{x^2-y^2}$ and d_{xy} orbitals which are somewhat tilted because the plane of the Ti atoms is not a symmetry plane. The single band at Γ is slightly higher in energy than the doubly-degenerate pair because of the slight rhombohedral distortion. The upper, doubly degenerate, Te-based bands are built from the Te p_x and p_y orbitals. Having identified the nature of these levels it is immediately clear that the Te-based doubly degenerate set is higher in energy for the PBE-type calculation. This means that, in the absence of Ti-Te hybridization, the Te p_x/p_y valence bands would raise up to higher energies at Γ than in the HSE06-type calculations. Consequently, when the hybridization is switched on, a larger number of electron and hole carriers is induced. Indeed, a careful look at the band structures in Fig. 4 shows that there is a significantly larger overlap between the top of the valence band around Γ and the bottom of the conduction band at M for the PBE functional than for HSE06. We note that the PBE-type band structure for single-layer $TiSe_2$, which provides a satisfactory description of the relative stability of the undistorted and 2×2 CDW in this system [13, 19], shows exactly the same topology and particularly, the same band ordering as the HSE06 band structure of Fig. 4b.

As soon as one moves along the Γ-M line (i.e. along the a^* direction), the only symmetry element preserved is the symmetry plane perpendicular to the layer and going along the a^* direction. One of the two Ti-based doubly degenerate levels at Γ and the Ti d_{z^2} mix and interact with one of the Te p bands near Γ leading to the slowly descending band from Γ-M which is associated with the electron pockets near M. With the local system of axes mentioned above, the crystal orbitals around M are almost exclusively made of tilted Ti $d_{x^2-y^2}$ orbitals (i.e. a mixing of Ti $d_{x^2-y^2}$ and Ti d_{z^2} which leads to the tilting of the orbital) exactly as we recently reported for the $TiSe_2$ single-layers [13]. We refer the reader to this work for a detailed analysis of the nature of the band structure which entirely applies to the HSE06 one reported in Fig. 4b.

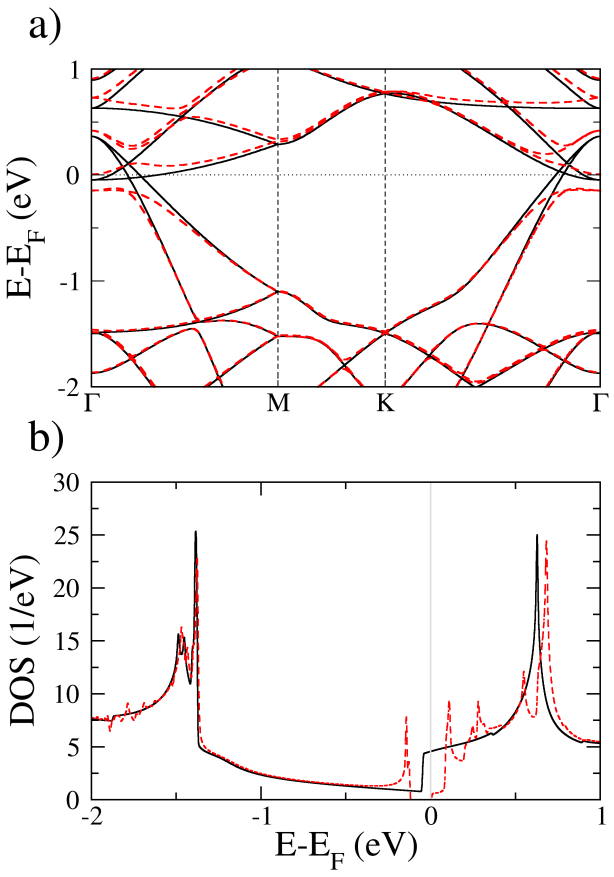

Figure 5. HSE06 band structure (a) and Density of States (DOS) (b) for single-layer $TiTe_2$. Broken red lines correspond to the 2×2 CDW structure and black continuous lines to the undistorted structure. The bands are represented in the BZ of the 2×2 structure and therefore are folded with respect to that in Fig. 1b. The origin of the energy scale is the Fermi level of the undistorted structure.

The HSE06 band structure and density of states for both the undistorted and the 2×2 CDW structures are reported in Figs. 5. As shown in both figures the stabilizing 2×2 CDW distortion opens a gap at the Fermi level. The analysis of the nature and origin of the distortion goes along the same lines presented in detail in our recent work for the $TiSe_2$ single-layer and will not be repeated here [13]. However, we note that the non-activated conductivity is kept in single-layer $TiTe_2$ below the CDW transition temperature [8] so that no gap should occur at the Fermi level. Consequently, the HSE06 calculations exaggerate the tendency towards the transition. As mentioned above, the PBE calculations suggest that under reasonable tensile strain a 2×2 CDW is favored without the development of a band gap. Only when the strain is relatively large (i.e. around 5-6%, see Fig. 2) a

band gap really opens. The HSE06 band structure of Fig. 5a is similar to that in Fig. 2c corresponding to a 6% tensile strength. We believe that the HSE06 functional exaggerates the stability of the 2×2 CDW and that the real situation concerning the weaker stabilization of the CDW phase and the lack of a full bandgap opening would rather correspond to that of the PBE functional with a moderate tensile strain. This observation, together with previous results on bulk $TiSe_2$ [20] suggest that a predictive description of these TiX_2 systems is attainable by using the HSE06 functional and tuning the actual contribution of the exact exchange. However, from the viewpoint of the physical origin of the CDW we do not find any noticeable difference with the previously reported analysis of the 2×2 CDW instability of $TiSe_2$ single-layers.

To further assess our conclusion we carried out HSE06 calculations for a $TiTe_2$ double-layer. Two single-layers with the optimized structure were placed with the interlayer bulk distance. The stabilization energy of the 2×2 CDW is reduced to practically one-half the value in the single-layer. Taking into account the small (and exaggerated) value for the single-layer, the driving force for the 2×2 CDW distortion in the $TiTe_2$ double-layer must be extremely small or most likely nil, as experimentally found.

Our study points out an interesting possibility. Since tensile strain has been found to be a useful technique to induce modifications in single-layer or few-flake materials [25, 26, 27, 28], it is possible that the 2×2 CDW can be induced in double-layers or triple-layers of $TiTe_2$ by using a small tensile strain.‡ Another useful hint provided by our study is that the 2×2 CDW in single-layer $TiTe_2$ may be more stable and result with a band gap under tensile strain or may be suppressed under a slight compresive strain.

3. Conclusions

A density functional theory study concerning the origin of the 2×2 CDW distortion recently reported experimentally for single-layer $TiTe_2$ has been carried out. This report is surprising because neither double-layer nor bulk $TiTe_2$ exhibit the 2×2 distortion and a PBE-based DFT study predicts that the undistorted structure is also more stable for the single-layer. Our study shows that, whereas calculations employing the semi-local functional PBE favor the undistorted structure, the hybrid functional HSE06 correctly predict the 2×2 distortion. However, the HSE06 calculations seem to exaggerate the stability of the distorted phase and, as a consequence, a noticeable band gap of more than 0.1 eV is induced at the Fermi level. This is in contrast with the metallic character of the $TiTe_2$ single-layers below the transition temperature. Interestingly, PBE type calculations for the case where the single-layer is subject to a slight tensile strain also favor the 2×2 distortion while keeping the semimetallic overlap. The study suggests that the magnitude of the semimetallic overlap is a key factor controlling the tendency towards the distortion and consequently only functionals describing such overlap very accurately can provide a truly predictive description of the electronic structure.

According to the present study the mechanism of the CDW instability in single-layer $TiTe_2$ seems to be the same phonon mediated mechanism acting for single-layer $TiSe_2$[13] although now the driving force is smaller and the semimetallic character is kept below the transition temperature. As mentioned above, the magnitude of the semimetallic overlap seems to be one of the key factors in controlling the likeliness of the 2×2 CDW. Taking into account that the overlap should increase in these TiX_2 systems when the number of short Te...Te contacts increase or when they become stronger, the overlap should increase from single-layers to bulk and from X=S to X=Te. Since the instability is not observed in bulk TiS_2 nor in double-layer $TiTe_2$, it seems that only a relatively narrow range of semimetallic overlaps is associated with the instability. In this respect, a significant result of the study is that tensile strain stabilizes the 2×2 CDW distortion in single-layer $TiTe_2$. This could be used to induce the instability in double- or triple-layers of $TiTe_2$ which in the absence of strain remain undistorted, to induce a stronger distortion leading to the creation of a band gap in single-layer $TiTe_2$ or most likely to suppress the 2×2 CDW under a small compression. Such studies could provide useful insight on the CDW mechanism of group IV 1*T*-TiX_2 phases.

This work was supported by Spanish MINECO (Grants FIS2015-64886-C5-3-P and FIS2015-64886-C5-4-P, and the Severo Ochoa Centers of Excellence Program under Grants SEV-2013-0295 and SEV-2015-0496), Generalitat de Catalunya (Grant 2017SGR1506 and the CERCA Programme) and by the European Union H2020-EINFRA-5-2015 MaX Center of Excellence (Grant No. 676598).

Appendix A. Computational details

The geometrical optimizations, electronic and phononic band structures were carried out using a numerical atomic orbitals density functional theory (DFT) [31,

‡ Note that tensile strain has been shown to decrease the semimetallic overlap and eventually lead to a band gap without changing the size of the unit cell both in single-layer [29] and bulk 1*T*-TiS_2) [30].

32] approach implemented in the SIESTA code [33, 34]. The Perdew-Burke-Ernzerhof (PBE) functional was used to account for the exchange-correlation energy [21]. The core electrons have been replaced by norm-conserving scalar relativistic pseudopotentials [35] factorized in the Kleinman-Bylander form [36]. We include the $3p$ shell of Ti explicity in the valence, as semicore states. We have used a split-valence double-ζ basis set including polarization functions [37]. The non-linear core-valence exchange-correlation scheme [38] was used for all elements. In the direction normal to the single-layer we chose a vacuum space of 50 Å in order to avoid possible interactions between the layer and its images. In the case of geometrical optimization calculations, the atomic coordinates were relaxed until the forces on them were below 10^{-5} eV/Å. In all calculations, we use a cutoff of 2500 Ry for the real space integrals, and a tolerance of 10^{-7} and 10^{-6} eV on the density matrix and the total energy, respectively, for the convergence of the SCF cycle. To sample the Brillouin cell for the electronic states, a Monkhorst-Pack [39] k-point grid of 300×300×1 was used for the undistorted minimum cell and it was scaled accordingly where supercell calculations were performed.

All HSE06 hybrid functional [22, 23] calculations were performed using the VASP code [40]. Core electrons were treated by means of the projector augmented wave method [41, 42] including semicore states for Ti. We used a planewave basis set with an energy cutoff of 330 eV. A Monkhorst-Pack [39] k-point grid of 24×24×1 was used to sample the Brillouin zone.

References

[1] Rossnagel K 2011 *J. Phys.:Condens. Matter* **23** 213001
[2] Wilson J, Di Salvo F and Mahajan S 1975 *Adv. Phys.* **24** 117–201
[3] Castro Neto A H 2001 *Physical Review Letters* **86** 4382
[4] Noat Y, Silva-Guillén J A, Cren T, Cherkez V, Brun C, Pons S, Debontridder F, Roditchev D, Sacks W, Cario L, Ordejón P, García A and Canadell E 2015 *Phys. Rev. B* **92**(13) 134510
[5] Bhimanapati G R, Lin Z, Meunier V, Jung Y, Cha J, Das S, Xiao D, Son Y, Strano M S, Cooper V R, Liang L, Louie S G, Ringe E, Zhou W, Kim S S, Naik R R, Sumpter B G, Terrones H, Xia F, Wang Y, Zhu J, Akinwande D, Alem N, Schuller J A, Schaak R E, Terrones M and Robinson J A 2015 *ACS Nano* **9** 11509–11539
[6] Ugeda M M, Bradley A J, Zhang Y, Onishi S, Chen Y, Ruan W, Ojeda-Aristizabal C, Ryu H, Edmonds M T, Tsai H Z, Riss A, Mo S K, Lee D, Zettl A, Hussain Z, Shen Z X and Crommie M F 2016 *Nature Physics* **12** 92
[7] Sugawara K, Nakata Y, Shimizu R, Han P, Hitosugi T, Sato T and Takahashi T 2016 *ACS Nano* **10** 1341–1345
[8] Chen P, Pai W W, Chan Y H, Takayama A, Xu C Z, Karn A, Hasegawa S, Chou M Y, Mo S K, Fedorov A V and Chiang T C 2017 *Nature Communications* **8** 516
[9] Xi X, Zhao L, Wang Z, Berger H, Forró L, Shan J and Mak K F 2015 *Nature Nanotechnology* **10** 765–769
[10] Li L J, O'Farrell E C T O, Loh K P, Eda G, Özyilmaz B and Castro-Neto A H 2016 *Nature* **529** 185
[11] Chen P, Chan Y H, Fang X Y, Zhang Y, Chou M, Mo S K, Hussain Z, Fedorov A V and T-C C 2015 *Nature Communications* **6** 8943
[12] Silva-Guillén J A, Ordejón P, Guinea F and Canadell E 2016 *2D Materials* **3** 035028
[13] Guster B, Canadell E, Pruneda M and Ordejón P 2018 *2D Materials* **5** 025024
[14] de Boer D K G, van Bruggeb C F, Bus G W, Coehoorn R, Haas C and Sawatzky G A 1984 *Phys. Rev. B* **29** 6797
[15] Koike Y, Okamura O, Nakanomyo T and Fukase T 1983 *J. Phys. Soc. Jpn.* **52** 597
[16] Allen P B and Chetty N 1994 *Phys. Rev. B* **50** 14855
[17] Di Salvo F J, Moncton D E and Waszczak J V 1976 *Phys. Rev. B* **14** 4321–4328
[18] Chen P, Chan Y H, Wong M H, Fang X Y, Chou M Y, Mo S K, Hussain Z, Fedorov A V and Chiang T C 2016 *Nano Lett.* **16** 6331–6336
[19] Singh B, Hsu C H, Tsai W F, Pereira V M and Lin H 2017 *Phys. Rev. B* **95** 245136
[20] Hellgren M, Baima J, Bianco R, Calandra M Mauri F and Wirtz L 2017 *Phys. Rev. Lett.* **119** 176401
[21] Perdew J P, Burke K and Ernzerhof M 1996 *Physical Review Letters* **77** 3865–3868
[22] Heyd J, Scuseria G E and Ernzerhof M 2003 *J. Chem. Phys.* **118** 8207–8215
[23] Krukau A V, Vydrov O A, Izmaylov A F and Scuseria G E 2006 *The Journal of Chemical Physics* 224106
[24] Arnaud Y and Chevreton M 1981 *J. Sol. State Chem.* **39** 2230
[25] Choi S M, Jhi S H and Son Y W 2010 *Nano Lett.* **10** 3486–3489
[26] Johary P and Shenoy U B 2012 *ACS Nano* **6** 5449–5456
[27] Biele R, Flores E, Ares J R, Sánchez C, Ferrer I J, Rubio-Bollinger G, Castellanos-Gomez A and D'Agosta R 2018 *Nano Research* **11** 225–232
[28] Roldán R, Chirolli L, Prada E, Silva-Guillén J A, San-Jose P and Guinea F 2017 *Chem. Soc. Rev.* **46** 4387–4399
[29] Xu C, Brown P A and Shuford K L 2015 *RSC Adv.* **5** 83876
[30] Samanta A, Pandey T and Dingh A K 2014 *Phys. Rev. B.* **90** 174301
[31] Hohenberg P and Kohn W 1964 *Physical Review* **136** B864–B871
[32] Kohn W and Sham L J 1965 *Physical Review* **140** A1133–A1138
[33] Soler J M, Artacho E, Gale J D, García A, Junquera J, Ordejón P and Sánchez-Portal D 2002 *Journal of Physics: Condensed Matter* **14** 2745–2779
[34] Artacho E, Anglada E, Diéguez O, Gale J D, García A, Junquera J, Martin R M, Ordejón P, Pruneda J M, Sánchez-Portal D and Soler J M 2008 *Journal of Physics: Condensed Matter* **20** 064208
[35] Troullier N and Martins J L 1991 *Physical Review B* **43** 1993–2006
[36] Kleinman L and Bylander D M 1982 *Physical Review Letters* **48** 1425–1428
[37] Artacho E, Sánchez-Portal D, Ordejón P, García A and Soler J M 1999 *Physica Status Solidi (b)* **215** 809–817
[38] Louie S G, Froyen S and Cohen M L 1982 *Physical Review B* **26** 1738–1742
[39] Monkhorst H J and Pack J D 1976 *Physical Review B* **13** 5188–5192
[40] Kresse G and Furthmüller J 1996 *Physical Review B* **54** 11169–11186
[41] Blöchl P E 1994 *Physical Review B* **50** 17953
[42] Kresse G and Joubert D 1999 *Physical Review B* **59** 1758